Energy 90 (2015) 1152–1162

Contents lists available at ScienceDirect

Energy

journal homepage: www.elsevier.com/locate/energy

Effects of natural gas compositions on CNG (compressed natural gas) reciprocating compressors performance

Mahmood Farzaneh-Gord [a], Amir Niazmand [a], Mahdi Deymi-Dashtebayaz [b, *], Hamid Reza Rahbari [a]

[a] The Faculty of Mechanical Engineering, Shahrood University of Technology, Shahrood, Iran
[b] Faculty Member of Mechanical Engineering, Hakim Sabzevari University, Sabzevar, Iran

ARTICLE INFO

Article history:
Received 27 December 2014
Received in revised form
10 May 2015
Accepted 7 June 2015
Available online 10 July 2015

Keywords:
Reciprocating natural gas compressor
Natural gas composition
Thermodynamic modeling
AGA8 equation

ABSTRACT

The aim of the current work is to investigate the effects of natural gas compositions on reciprocating compressor performance numerically. A numerical model has been built based on first law of thermodynamics, mass balance, AGA8 EOS (Equation of State) and thermodynamics relationships. The model could predict compressor parameters (pressure, temperature, mass flow rate, mass and valves motions) at various crank angles and cylinder volume. For validation, the numerical results are compared with previous experimental values and good agreement is encountered. The impact of key parameters such as: clearance, angular speed and molecular weight of natural gas have been investigated on the compressor performance. The results show that, for natural gas with higher molecular weight, suction valve opening time is less than natural gas with lower molecular weight. Also, the consuming indicated work per cycle for natural gas with lower molar weight (Khangiran composition with 98% methane) is approximately 50 kJ/kg more than higher molar weight (Ghasoo gas with 79% methane).

1. Introduction

Reciprocating compressors are utilized extensively in various industries such as: power plants and refineries, refrigeration systems and CNG stations (Compressed Natural Gas stations). The key feature of these compressors is high pressure ratio achievement.

A reciprocating compressor is the heart of any CNG station. In CNG station, natural gas must be compressed from the distribution pipeline pressure (about 0.5 MPa) to a much higher value (20 MPa–25 MPa) [1,2]. This pressure rise is done by employing a multi-stage compressor (three or four stages). A major part of the initial and current costs of CNG stations are dependent on reciprocating compressor. Also, one of the greatest difficulties in CNG stations is high work required for compressing natural gas [2]. Accurate modeling of CNG compressors could improve design parameters that lead to efficiency enhancement and required work reduction.

There are two main methods for simulating reciprocating compressor. These are global and differential methods, which in both methods; the variables depend on crank angle [3]. Stouffs et al. [3] presented a global method for studying reciprocating compressors performance. They calculated the effective parameters such as: the indicated work per unit mass and volumetric effectiveness. In another work, Armaghani et al. [4] developed a simple global method to investigate the effect of engine speed on thermodynamics properties of an air reciprocating compressor. Their method was able to predict the volumetric effectiveness, the specific work and the indicated efficiency of the air typical compressor at different operating pressure ratios. Farzaneh-Gord et al. [5,6] have also developed a thermodynamic model for analyzing reciprocating compressors. In the study, they presented a method for determining optimized design parameters of an air compressor.

Casting et al. [7] presented a dynamic simulation and experimental validation of reciprocating compressors. Their research showed that the dead volumetric ratio and a friction factor have influences on volumetric efficiency and effective efficiencies respectively. Porkhial et al. [8] have developed a numerical program for compressors and compared the results with numerical studies by applying mass and energy balances. Pe'rez-Segarra et al. [9] did a detailed thermodynamic analysis of reciprocating compressors.

* Corresponding author.
E-mail addresses: mgord@shahroodut.ac.ir, mahmood.farzaneh@yahoo.co.uk (M. Farzaneh-Gord), amir_omid86@yahoo.com (A. Niazmand), m.deimi@hsu.ac.ir, meh_deimi@yahoo.com (M. Deymi-Dashtebayaz), rahbarihamidreza@yahoo.com (H.R. Rahbari).

http://dx.doi.org/10.1016/j.energy.2015.06.056
0360-5442/

They focused on the volumetric efficiency, the isentropic efficiency, and the combined mechanical–electrical efficiency.

Elhaj et al. [10] have presented a numerical analysis for predictive behavior of two-stage reciprocating compressor. Winandy et al. [11] presented a simple model for investigating reciprocating compressor performance. In their study, the main objective was the calculating the required work and discharge temperature. Also Ndiaye et al. [12] presented a dynamic model of a hermetic reciprocating compressor in on-off cycling operation. Enrico Da Riva et al. [13] calculated the performance of a semi-hermetic reciprocating compressor that has been installed in a heat pump for generating 100 kW heating capacity. Damle et al. [14] presented a numerical model to foretell the thermodynamic parameters and power consumption of the compressor during compression process. Also Negrao et al. [15] studied the behavior of reciprocating compressor based on a semi-empirical numerical simulation. In the study, they calculated the variation of power consuming based on producer details. Yuan Ma et al. [16] presented a numerical program for analyzing the valves movement of CO_2 compressor. They compared the numerical result with the experimental values.

Natural gas is a mixture of various hydrocarbon molecules such as methane (CH_4), ethane (C_2H_6), propane (C_3H_8), butane (C_4H_{10}) and inert diluents such as molecular nitrogen (N_2) and carbon dioxide (CO_2). Several parameters affect the natural gas composition variations which is including geographical source, time of year, and treatments applied during production or transportation [17,18]. Therefore, natural gas does not describe a single type of fuel or a narrow range of characteristics [19,20]. For accurate studying natural gas process, it is essential to know thermodynamic properties of natural gas. To achieve this goal, AGA8 equation of state (EOS) could be employed [21,22]. American Gas Association has provided the AGA8 equation of state [21,23]. It incorporates both theoretical and empirical elements. This has provided the correlation with the degree of numerical flexibility needed to achieve high accuracy for the compressibility factor and density of natural gas for custody transfer.

Reciprocating compressors is also employed in NG (Natural Gas) industry such as CNG stations. By modeling NG reciprocating compressors, it is possible to study effects of various parameters on their efficiency and to identify the optimum design parameters. The improvement of design parameters of these compressors leads to higher compressor performance. Also by modeling these compressors, it is possible to diagnosis possible defect which decrease compressor performance.

The objective of this work is to study effects of natural gas compositions on the reciprocating compressors performance thermodynamically. The thermodynamic simulation is based on first law of thermodynamics, conservation of mass and considering natural gas as a real gas mixture. In the current study, four typical natural gas compositions including: Khangiran, Kangan, Pars and Ghasho has been selected for investigation. These gases have been selected due to highest different in their compositions among all Iranian pipeline natural gases. The thermodynamic properties of natural gas have been calculated based on AGA8 EOS. The modelling could predict thermodynamic properties such as: in-cylinder pressure, temperature, mass flow rate and mass at various crank angles and cylinder volume for various natural gas compositions. Also, the effects of the compressor characteristics, such as angular speed and clearance on the input work have been investigated.

2. Natural gas compositions

Natural gas is a mixture of several components with various properties. Therefore, its thermodynamics properties are depended on its components. To obtain its properties accurately, the effect of the gas compositions must be also considered. Here, the AGA8 EOS has been employed (See Appendix A) to compute the properties. Table 1 shows the molar present of four typical compositions employed in this study. These gases are extracted from the various regions within Iran [24]. These NG have been selected as case studies due to highest different in their compositions among Iranian natural gases fields. Since it may be necessary to increase the pressure of sour natural gas, the Ghashoo gas composition (as sour gas with H_2S about 6.32 present) was also considered.

Table 1
Mole fraction of natural gas extracted from various region of Iran [24].

Component	Mole fraction (%)			
	Khangiran	Kangan	Pars	Ghashoo
CH_4	98.6	90.04	87	79.08
C_2H_6	0.59	3.69	5.4	0.91
C_3H_8	0.09	0.93	1.7	0.36
i-C_4H_{10}	0.02	0.2	0.3	0.09
n-C_4H_{10}	0.04	0.29	0.45	0.18
i-C_5H_{12}	0.02	0.14	0.13	0.08
n-C_5H_{12}	0.02	0.08	0.11	0.07
n-C_6H_{14}	0.07	0.14	0.07	0.069
C_7^+	0	0.01	0.03	0
N_2	0.56	4.48	3.1	5.14
CO_2	0	0	1.85	7.08
H_2S	0	0	0	6.32
Molecular weight (kg/kmol)	16.3148	17.794	18.5801	20.6887

3. Methodology

Fig. 1 shows a schematic diagram of a typical NG reciprocating compressor with spring type suction and discharge valves. The connecting rod converted the reciprocating movement of piston to the rotary movement of crankshaft. NG within cylinder is assumed as a lump open thermodynamic system. It is also assumed that no leakage take place. The governing equation for thermodynamic modelling of reciprocating compressor is presented in the following sections.

3.1. First law equation

To develop a numerical model, the first law of thermodynamics, conservation of mass and AGA8 equation of state have been employed. As shown in Fig. 1, the interior of the cylinder is

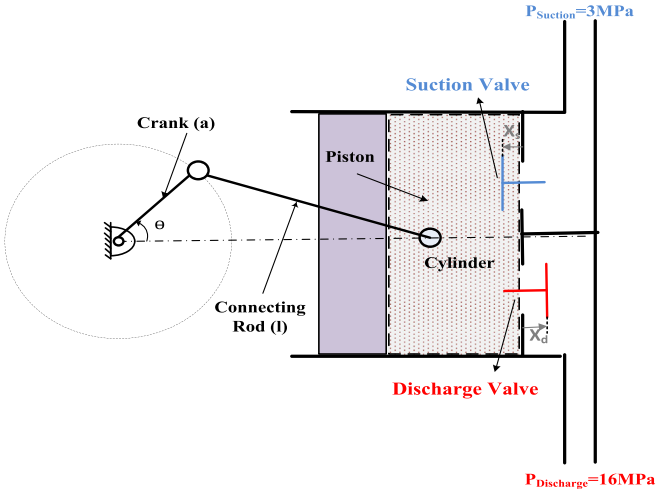

Fig. 1. A schematic of reciprocating compressor.

considered as a control volume. The boundaries of control volume consist of the cylinder wall, cylinder head and piston end face. The first thermodynamic law could be written as follow:

$$\dot{Q}_{cv}+\sum \dot{m}_s\left(h_s+\frac{Ve_s^2}{2}+gz_s\right)=\sum \dot{m}_d\left(h_d+\frac{Ve_d^2}{2}+gz_d\right)+\frac{d}{dt}\left[m\left(u+\frac{Ve^2}{2}+gz\right)\right]_{cv}+\dot{W}_{cv} \tag{1}$$

where $\dot{W}, h, u, Ve, \dot{m}, z, g$ and $\dot{Q}$ are work rate, enthalpy, internal energy, velocity, mass flow rates, altitude, acceleration of gravity and heat transfer respectively. Also s, d and cv subscripts stand for suction, discharge and control volume conditions. By ignoring variations of kinetic and potential energies, the equation (1) could be simplified as follow:

$$\frac{dQ_{cv}}{dt}+\frac{dm_s}{dt}h_s=\frac{dm_d}{dt}h_d+\frac{d}{dt}(mu)_{cv}+\frac{dW_{cv}}{dt} \tag{2}$$

The variation in work can be calculated as follow:

$$\frac{dW_{cv}}{dt}=P_{cv}\frac{dV_{cv}}{dt} \tag{3}$$

In equation (3) P and V are pressure and volume respectively. By replacing equation (3) in equation (2), the equation (4) can be acquired:

$$\frac{dQ_{cv}}{dt}+\frac{dm_s}{dt}h_s=\frac{dm_d}{dt}h_d+\frac{d}{dt}(mu)_{cv}+P_{cv}\frac{dV_{cv}}{dt} \tag{4}$$

Also, differentiating respect to time could be converted to crank angle by considering the following equation:

$$\frac{d}{dt}=\frac{d}{d\theta}\times\frac{d\theta}{dt}=\omega\frac{d}{d\theta} \tag{5}$$

Where ɵ and ω are the crank angle and rotational speed of the crank shaft respectively. Finally, the first law of thermodynamic could be modified as below:

$$\frac{dQ_{cv}}{d\theta}+\frac{dm_s}{d\theta}h_s=\frac{dm_d}{d\theta}h_d+\frac{d}{d\theta}(mu)_{cv}+P_{cv}\frac{dV_{cv}}{d\theta} \tag{6}$$

3.2. Piston motion equation

The accurate instantaneous piston displacement from top dead center in terms of the crank angle could be presented as [25]:

$$x(\theta)=\frac{S}{2}\left[1-\cos\theta+\frac{L}{a}\left(1-\sqrt{\left(1-\left(\frac{a}{L}\sin\theta\right)^2\right)}\right)\right] \tag{7}$$

where a, L and S are lengths of rod, crank and stroke respectively. The momentarily volume of cylinder is obtained as [25]:

$$V_{cv}(\theta)=A_{cv}\times S(\theta)+V_0 \tag{8}$$

where $V_0$is the dead volume.

3.3. Conservation of mass

Considering the control volume of Fig. 1, the conservation of mass equation could be written as follows:

$$\frac{dm_{cv}}{dt}=\dot{m}_s-\dot{m}_d \tag{9}$$

By replacing equation (5) in equation (9), the conservation of mass equation could be rewritten as:

$$\frac{dm_{cv}}{d\theta}=\frac{1}{\omega}(\dot{m}_s-\dot{m}_d) \tag{10}$$

where $\dot{m}_s$ and $\dot{m}_d$ are the mass flow rates through suction and discharge valves respectively, which are computing from following equations [26,27]:

$$\dot{m}_s=\begin{cases}C_{ds}\rho_s A_s\sqrt{\dfrac{2(P_s-P_{cv})}{\rho_s}} & \text{for } P_s>P_{cv} \text{ and } x_s>0\\ -C_{ds}\rho_{cv}A_s\sqrt{\dfrac{2(P_{cv}-P_s)}{\rho_{cv}}} & \text{for } P_{cv}>P_s \text{ and } x_s>0\end{cases} \tag{11}$$

$$\dot{m}_d=\begin{cases}C_{dd}\rho_{cv}A_d\sqrt{\dfrac{2(P_{cv}-P_d)}{\rho_s}} & \text{for } P_{cv}>P_d \text{ and } x_d>0\\ -C_{dd}\rho_d A_d\sqrt{\dfrac{2(P_d-P_{cv})}{\rho_d}} & \text{for } P_d>P_{cv} \text{ and } x_d>0\end{cases} \tag{12}$$

where A_s and A_d are the flow areas through the suction and discharge valves. They are obtained by:

$$\begin{aligned}A_s&=2\pi x_s r_s\\ A_d&=2\pi x_d r_d\end{aligned} \tag{13}$$

where x_s and x_d are the suction and discharge displacement from the closed valve position, and, r_s and r_d are radius of suction and discharge valves respectively.

Due to non-ideality of the valve, it does not shut down instantaneously as soon as a negative pressure difference is created from its reference motion, turn the direction and shut the opening. Coefficient of C_{ds} and C_{dd} account these non-ideality of valves.

3.4. Valve movement equation

The valve dynamic equations are derived based on the following assumption;

(i) The valve is considered as a single degree of freedom system.
(ii) The valve plate is rigid.
(iii) The valve displacement is restricted by a suspension device.

Reference point of motion is the closed position of the valve. The valves do not have any negative displacement. Considering the forces acting on the valve plates, the general equation of motion for a valve plate is then given by Ref. [28]:

$$\frac{d^2x_s}{d\theta^2}=\frac{1}{m_s\omega^2}\left\{-k_s x_s+C_{fs}A_s(P_s-P_{cv})+F_{ps}\right\} \quad \text{for } x_s>0 \text{ and } x_s^{\max}>x_s \tag{14}$$

$$\frac{d^2x_d}{d\theta^2}=\frac{1}{m_d\omega^2}\left\{-k_d x_d+C_{fd}A_d(P_{cv}-P_d)+F_{pd}\right\} \quad \text{for } x_d>0 \text{ and } x_d^{\max}>x_d \tag{15}$$

where F_{ps} and F_{pd} are pre-load forces, that these forces are neglected respect to the other forces. Also m_s and m_d are masses

of suction and discharge, respectively. Coefficient of C_{fs} and C_{fd} account loss of the energy due to the orifice flow and these coefficients can be obtained from previous study [29].

3.5. Heat transfer equation

Heat transfer due to convection in compression chamber can be calculated for each crank angle from below equation [30–37]:

$$\frac{dQ}{d\theta} = \frac{\alpha A}{\omega}(T_{cv} - T_w) \tag{16}$$

where α, A, T_{cv} and T_w are the heat transfer coefficient, surface area in contact with the gas, the in-cylinder gas temperature and the wall temperature respectively. Adair et al. [30] observed that the cylinder wall temperature varies less than ±1 °F, as a result the wall temperature is assumed constant.

To calculate convective heat transfer coefficient, α, the Woschni correlation has been employed [31]. This correlation is originally derived for internal combustion engine. The correlation could also predict the heat transfer rate during compression stage of engine motion. Consequently, it could be used to model heat transfer in a reciprocating compressor. According to the correlation, the heat transfer coefficient is given by:

$$\alpha = 3.26D^{-0.2}P^{0.8}T^{-0.55}Ve^{0.8} \tag{17}$$

where, Ve and D are the characteristic velocity of gas and diameter of the cylinder respectively. According to Woschni correlation, the correlation characteristic velocity for a compressor without swirl is given as [31]:

$$Ve = 2.28Ve_p \tag{18}$$

where, Ve_p is average velocity of the piston.

3.6. Procedure for calculating thermodynamic properties

Clearly for obtaining in-control volume properties, in first step, the two independent thermodynamic properties should be calculated and then other thermodynamics properties could be computed. In this study, the two independent thermodynamic properties are density and internal energy. By using conservation of mass and first law of thermodynamic equations, density (or specific volume) and internal energy could are calculated firstly. Then, AGA8 EOS has been used for computing thermodynamic properties of natural gas mixture as real gas (See Appendix A). Farzaneh-Gord and Rahbari [23] have provided the detailed procedure of calculation natural gas thermodynamics properties.

4. Numerical procedure

As mentioned in the previous section, first law and conservation of mass equations are employed to calculate two independent thermodynamic properties. These equations are discretized as follow [25]:

$$\frac{u_{cv}^{j+1} - u_{cv}^{j}}{\Delta\theta} = \frac{1}{m_{cv^j}}\left\{\left(\frac{\Delta Q_{cv}}{\Delta\theta}\right)^j + h_s^j\left(\frac{\Delta m_s}{\Delta\theta}\right)^j - P_{cv^j}\left(\frac{\Delta V}{\Delta\theta}\right)^j - h_d^j\left(\frac{\Delta m_d}{\Delta\theta}\right)^j - \left(\frac{\Delta m_{cv^j}}{\Delta\theta}\right)u^j\right\} \tag{19}$$

$$\frac{\Delta m_{cv}}{\Delta\theta} = \frac{\dot{m}_s - \dot{m}_d}{\omega} \Rightarrow m_{cv}^{j+1} - m_{cv}^{j} = \Delta\theta\left(\frac{\dot{m}_s^j - \dot{m}_d^j}{\omega}\right) \Rightarrow m_{cv}^{j+1} = m_{cv}^{j} + \Delta\theta\left(\frac{\dot{m}_s^j - \dot{m}_d^j}{\omega}\right) \tag{20}$$

By using Runge-kotta method, the specific internal energy and m_{cv} are calculated from equations (19) and (20) for each crank angle. Finally by knowing in-cylinder volume, one could calculate density at each crank angle as:

$$\rho_{(\theta)}^{j+1} = \frac{m_{cv(\theta)}^{j+1}}{V_{cv(\theta)}^{j+1}} \tag{21}$$

These two thermodynamic properties (density and specific internal energy) are enough to identify other thermodynamic properties. For calculating pressure and temperature for each time step, thermodynamic table which formed based on AGA8 EOS, are used. The table is arranged according to internal energy (u) and density ($\rho_{(\theta)}$). Functions of pressure and temperature are prepared by Curve fitting method.

Fig. 2 shows the flowchart of extended AGA8 model. As illustrated in the figure, the input of the algorithm is internal energy, density and natural gas composition. These two thermodynamic properties (density and specific internal energy) are enough to identify the other thermodynamic properties (temperature, pressure).

The calculation continues until the crank angle is smaller than or equal to 360° (or $\theta \leq 360$).

The values of work and indicated work per in-control volume mass are also calculated as the following equations:

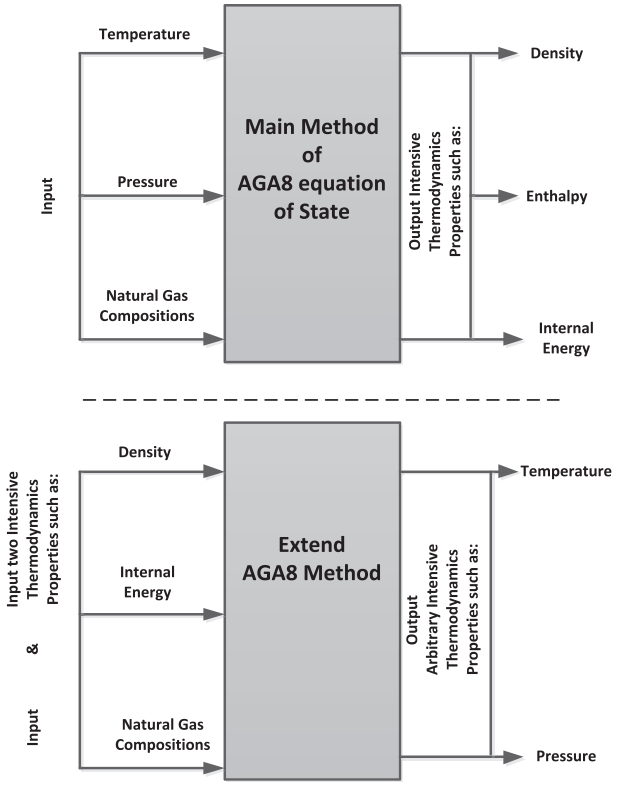

Fig. 2. Flowchart of extended AGA8 model.

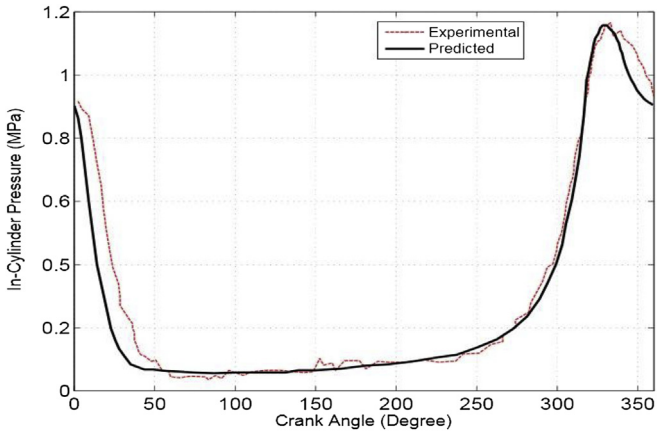

Fig. 3. Comparison between numerical and measured values [38] of cylinder pressure at $\omega = 1800$ rpm.

$$W = F \times \int P_d V = F \times \sum_{j=1}^{N} P_d^j V^j \tag{22}$$

$$W_{indicated} = \frac{1}{m_{cv}} \int P_d V = \frac{1}{m_{cv}} \sum_{j=1}^{N} P_d^j V^j \tag{23}$$

In which N and F are the number of steps and the frequency respectively. Frequency could be obtained as:

$$F = 2\pi \times \omega \tag{24}$$

5. Results and discussion

Firstly, for validation the numerical method, the numerical results have been compared with available experimental values [38]. Venkatesan et al. [38] reported in-cylinder parameters variation for a reciprocating air compressor experimentally. Fig. 3 compares the in-cylinder pressure variation between numerical results and experimental values [38]. For experimental values, the volume displaced by the piston is larger than the amount of air entering into the cylinder during suction period. The suction and discharge pressures are assumed constant in the numerical study. As a result, a decrease in cylinder pressure is anticipated for the experimented case. This could be observed in the figure. Similarly, the volume displaced by the piston is greater than the volume of air discharged through discharge port for the experimented case during discharge period. Therefore, an increase in cylinder pressure is anticipated. Table 2 presents a comparison between numerical and experimental values of peak pressure and volume flow rate. Generally, there are a good agreement between the measured and numerical values.

The remaining results are for a specific compressor with NG as working fluid. The basic specifications required for modeling the reciprocating NG compressor are listed in Table 3. This information includes the geometric properties and thermodynamic conditions. The effects of various parameters are also investigated in separated sections.

Table 2
Comparison between measured [38] and numerical value of two points pressure at $\omega = 1800$ rpm.

	Peak pressure (bar)	Free air delivered (liter/min)
Experimental [39]	11.58	277.4
Predicted	11.51	280.2
Error (%)	0.6	1.01

Table 3
Specifications of reciprocating NG compressor used for modeling.

Specification	Symbol	Value	Unit
Diameter of cylinder	D_{cyld}	15	cm
Stroke	S	10	cm
Bore	B	14.5	cm
Radius of suction port	R_s	2.96	cm
Radius of discharge port	R_d	4.33	cm
Suction port spring stiffness	k_s	16	N/mm
Discharge port spring stiffness	k_d	16	N/mm
Rotational speed	ω	900	rad/sec
Suction temperature	T_s	286	K
Suction pressure	P_s	3	MPa
Discharge pressure	P_s	16	MPa
Pressure ratio	P_s/P_d	5.33	–

Fig. 4 shows the variation of in-cylinder pressure for various natural gas compositions versus a) cylinder volume and b) crank angle. The modeling starts from TDC (Top Dead Center) where cylinder volume is same as clearance volume. By piston movement from TDC towards BDC (Bottom Dead Center), the cylinder volume is increasing and consequently pressure is reducing. For all natural gas compositions, graphs are coincidence until suction valve is opened. For all figures in this section (Figs. 5–9), once suction valve is opened suction process starts. The figure clearly shows the significantly of natural gas compositions on the pressure profiles.

Variation of in-cylinder temperature for various natural gas compositions versus a) cylinder volume and b) crank angle has been presented in Fig. 5. At the beginning of suction process,

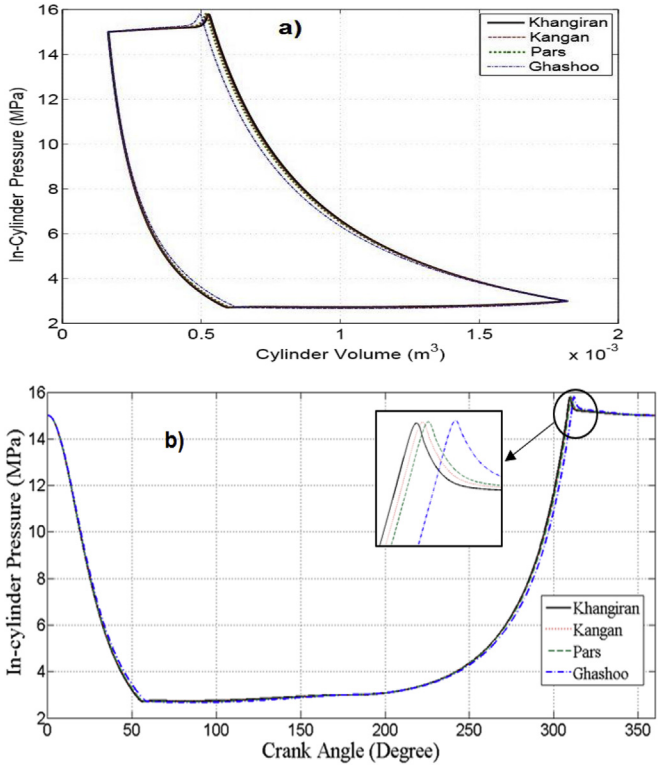

Fig. 4. Variation of in-cylinder pressure for various natural gas compositions versus a) cylinder volume and b) crank angle.

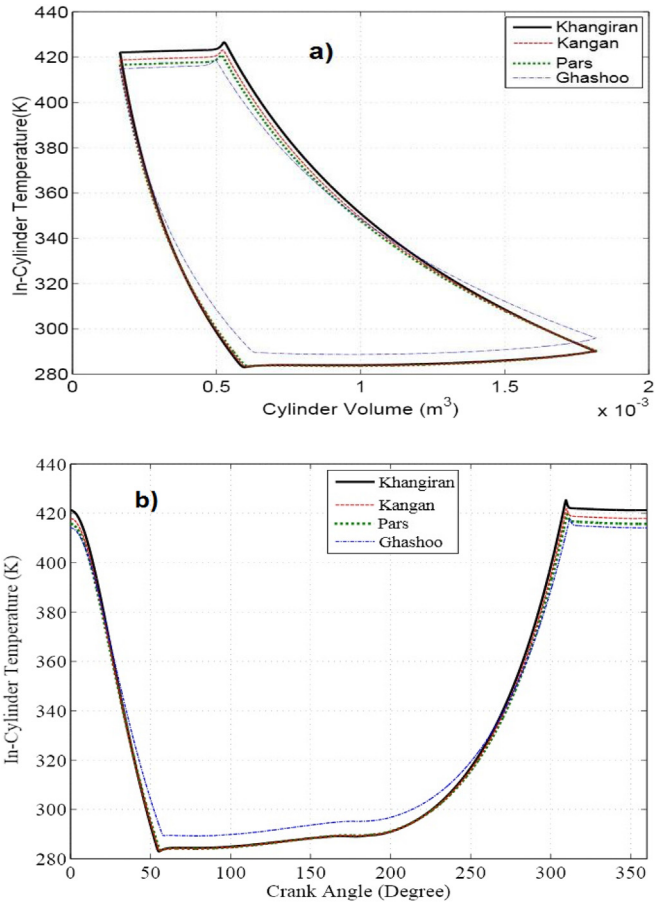

Fig. 5. Variation of in-cylinder pressure for various natural gas compositions versus a) cylinder volume and b) crank angle.

temperature decreases by suddenly entering high pressure NG into the cylinder. Then an increasing trend starts till half of the cycle. Temperature drop in suction process is mainly due to the specific volume decrement and Joule-Thomson effect. NG is a real gas with positive Joule–Thomson coefficient so temperature drop due to pressure drop is expected. As shown this figure, the final in-cylinder temperature is highest for the Kangiran gas composition with lowest molar weight (highest methane percentage).

Fig. 6 shows the variations of a) suction and b) discharge valves motion for various natural gas compositions versus crank angle. The figure illustrates that valves vibration happens during opening and closing time. As showed in this figure, with increasing the molecular weight of natural gas, the valves opening time increases.

Fig. 7 illustrates a) suction and b) discharge mass flow rates for various natural gas compositions versus crank angle. It could be realized that there is backward flow for suction valve. Note from the figure, the suction and discharge mass flow rates is highest for the Ghashoo gas composition with highest molar weight (lowest methane percentage). This is mainly due to higher density for such gas. The figure shows the significantly of natural gas compositions on the mass flow rate profiles.

Fig. 8 shows the variation of a) in-cylinder mass and b) density for various natural gas compositions as a function of crank angle. The mass of NG within cylinder are raised while the suction port is open. Then, it stays on a specific value for each natural gas composition during the compression process. By opening the

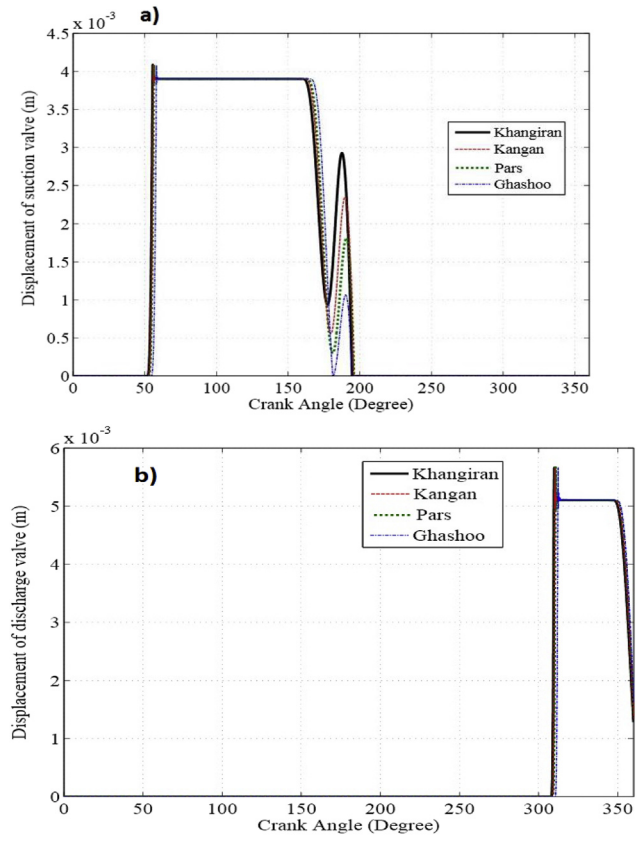

Fig. 6. Displacement of a) suction and b) discharge valves for various natural gas compositions versus crank angle.

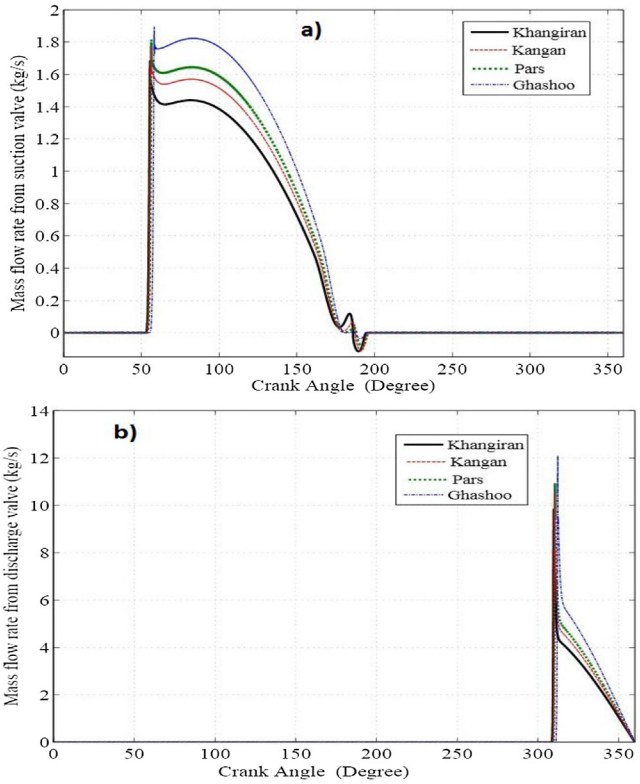

Fig. 7. a) Suction and b) discharge mass flow rates for various natural gas compositions versus crank angle.

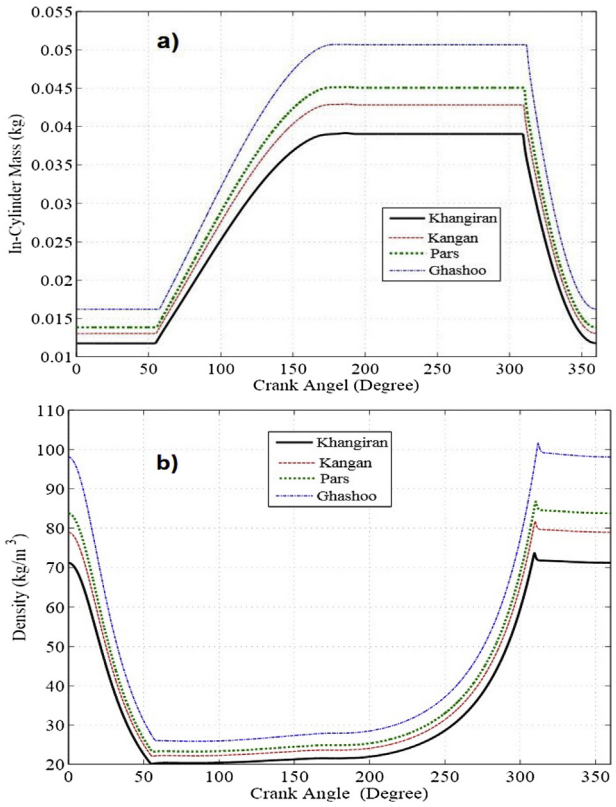

Fig. 8. Variation of a) In-cylinder mass and b) density for various natural gas compositions versus crank angle.

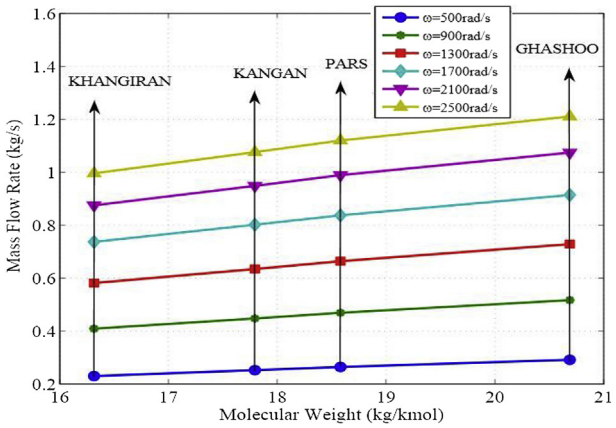

Fig. 9. Variation of mass flow rate vs. natural gas molecular weight in different angular speed.

discharge port, a sudden discharge happens at the beginning but it continues with a more balanced procedure afterwards. Also as expected (due to higher density), the in-cylinder mass of Ghasoo composition is higher comparing to other natural gas compositions. This again shows the significantly of natural gas compositions on the process. More explanation could be argued that the density of the NG is higher for low methane percentage comparing to the high methane composition. For this reason, the mass flow rate that entering control volume is higher for composition with low methane percentage and consequently, in-cylinder mass is higher for these compositions (for example Ghashoo).

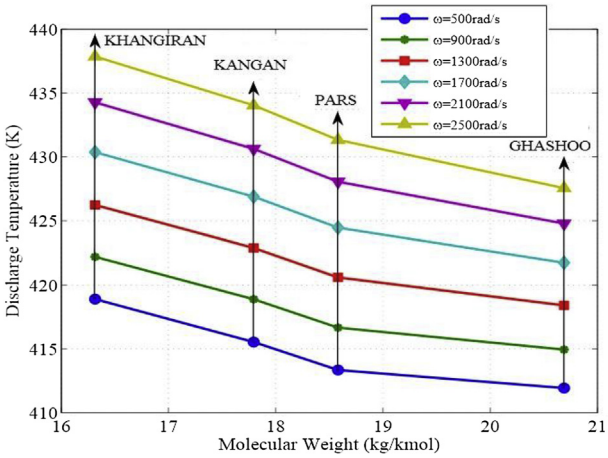

Fig. 10. Variation of mean discharge temperature vs. natural gas molecular weight in various angular speeds.

5.1. *Effect of angular speed on compressor performance for various natural gas compositions*

In this section, the effects of angular speed on compressor performance for various natural gas compositions are presented. The investigated angular speeds are between 500 rad/s to 2100 rad/s.

The variation of mass flow rate against various molar weights of natural gas is shown in Fig. 9. It should be noted, as molecular weight increases, the natural gas density increases too. It consequently increases the mass flow rate. It is evident that as the angular speed increases, the mass flow rate also increases. This can be explained by the relationship between angular speed and the number of cycle in same time. Increasing the angular speed increases the frequency and consequently the mass flow rate.

Fig. 10 shows the variation of mean discharge temperature against various molar weights of natural gas. Based on the figure, it is evident that with increasing the angular speed, the mean discharge temperature increases. This can be explained by the relation between angular speed and in-cylinder mass. With increasing angular speed, the in-cylinder mass in one cycle is reduced considerably. The more in-cylinder mass cause in-cylinder gas to cool less and consequently, the discharge temperature stays low for lower angular speeds. In other hand, with increasing molecular weight, the mean discharge temperature deceases. It is due to the higher density for natural gas with higher molecular weight. Considering on equation of state for a gas, for a constant pressure process, as density increases, the temperature will decrease.

Figs. 11 and 12 show the effects of angular speed on work and input indicated work per cycle for various natural gas compositions respectively. It could be realized, the consuming indicated work per cycle for NG with highest methane percentage is significantly higher than NG with lowest methane percentage. For example the consuming indicated work per cycle for Khangiran composition with 98% methane is about 50 kJ/kg higher than Ghasoo gas with 79% methane. With increasing molar mass, in-cylinder mass increases, however the in-cylinder pressure does not vary noticeably. This is reason for decreasing the indicated work per mass. As the indicated work is obtained by dividing work to one cycle mass flow, the indicated work in natural gas compositions with high methane percentage is higher than the low methane percentage compositions.

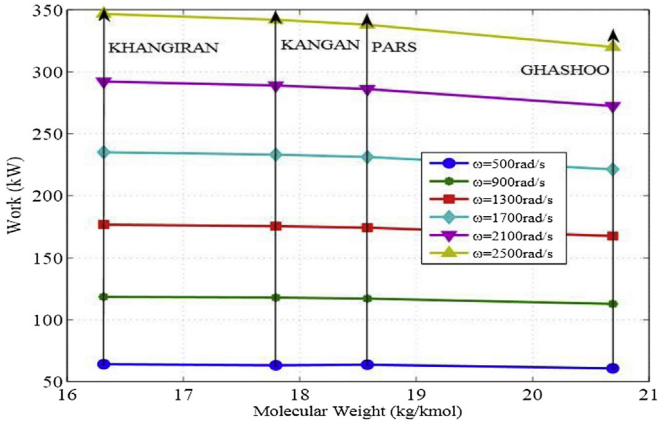

Fig. 11. Variation of work vs. natural gas molecular weight in various angular speeds.

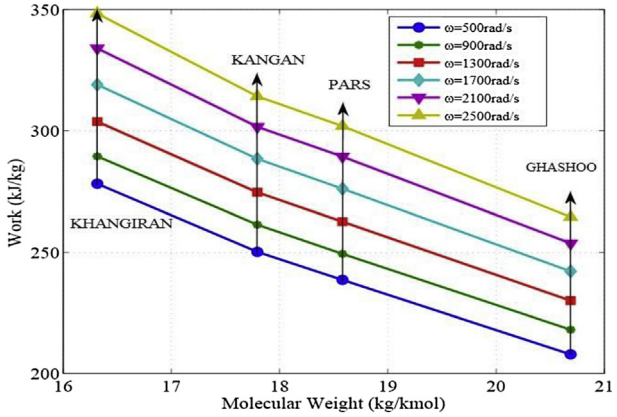

Fig. 12. Variation of indicated work per cycle vs. natural gas molecular weight in various angular speeds.

5.2. *Effect of clearance value on compressor performance for various natural gas compositions*

Due to various reasons such as the heat expansion of compressor pieces, exist of clearance in reciprocating compressor is unavoidable. To study effects of clearance value on compressor performance, clearances percent are varied among 7, 9, 11, 13 and 15 in this section. Fig. 13 shows the variation of mass flow rate against natural gas molecular weight for various clearance percentages.

Fig. 14 presents the variation of mean discharge temperature against natural gas molecular weight for various clearance percentages. As it is shown, the effect of clearance value on discharge temperature isn't much. For example, discharge gas temperature difference for clearances 7% and 15% is about 0.5 K. As molecular weight decreases, the discharge temperature of compressed gas is increased. As an example, temperature difference of expanded gas between clearances 7% and 15% just before suction process is 2.5 K.

Fig. 15 presents the influence of variation of clearance on work for various natural gas compositions. It could be realized, in similar angular speed, the consuming indicated work per cycle for NG with highest methane percentage is significantly higher than NG with the lowest methane percentage. For example, in similar clearance, the consuming work for Khangiran composition with 98% methane is about 5 kW higher than Ghasoo gas with 79% methane.

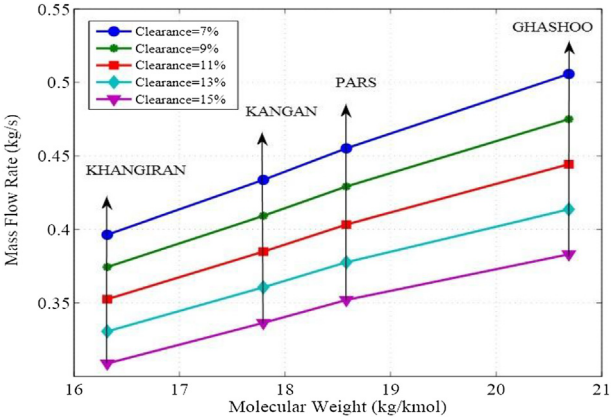

Fig. 13. Variation of mass flow rate vs. natural gas molecular weight in various clearances.

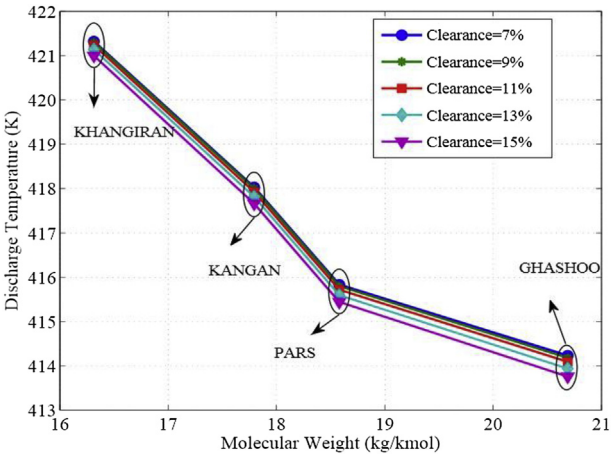

Fig. 14. Variation of discharge temperature vs. natural gas molecular weight in various clearances.

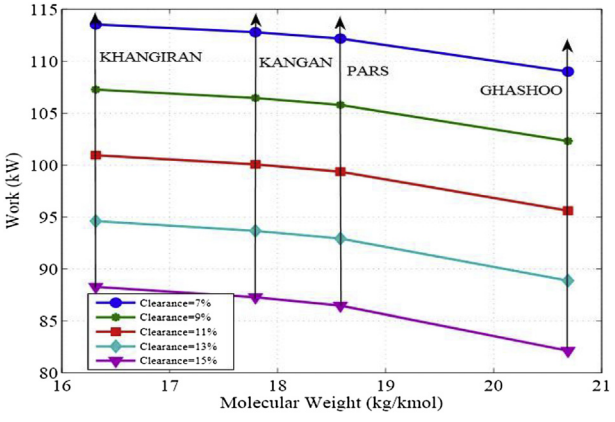

Fig. 15. Variation of work vs. natural gas molecular weight in various clearances.

Fig. 16 shows the indicated work in various clearances for various natural gas compositions. The results show that change in clearance doesn't have significant effects on the indicated work. In other hand, as it was evident in the previous figures, as the gas density increases, in-cylinder mass also increases. Therefore, based on Equation (23), in the same pressure and volume, increasing in-cylinder mass could be reduced indicated work.

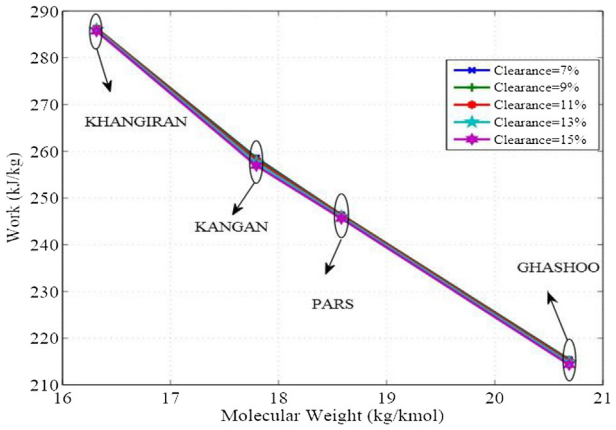

Fig. 16. Variation of indicated work per cycle vs. natural gas molecular weight in various clearances.

6. Conclusion

Natural gas compression processes are sometimes carried out by the reciprocating compressors in natural gas industries when high pressure ratio is required. Comprehension the demeanor of these compressors and inspecting effects of various parameters on their performance are attractive subject. Because of the diversity of NG compositions, the effect of the natural gas composition variation on the compressor performance is an important subject. Hence, in this study, the effects of natural gas composition variation on the compressor performance were evaluated.

The first laws of thermodynamics, mass conservation equation and AGA8 EOS have been employed as tools to investigate the effects of natural gas composition variation on performance of one stage CNG reciprocating compressors.

The effects of natural gas compositions variation on thermodynamic parameters such as: pressure, temperature, in-cylinder mass and mass flow rates were studied. The effects of various parameters such as: angular speed, clearance and natural gas compositions on required work per unit mass of gas are also investigated. The main results could be summarized as follows:

- For all natural gas compositions, as the angular speed increases, the required indicated work per cycle increases too.
- For various natural gas compositions, as the molecular weight increases, the valves opening time increases too.
- The mean discharge temperature for NG with lower molecular weight (higher present of methane) is more than NG with higher molecular weight (lower present of methane).
- The consuming work per cycle for Khangiran gas (with 98% methane) is significantly higher than the Ghasoo gas (with 79% methane).

Considering the above comments, one could conclude that the natural gas composition has significant effects on compressor performance and should be considered as an important parameter.

Acknowledgment

Authors would like to thank the officials in NIOPDC Company for financial support.

Appendix A. Real gas effect

To study the effect of real gas in simulations, AGA8 equation of state (EOS) has been used. It incorporates both theoretical and empirical elements. This has provided the correlation with the degree of numerical flexibility needed to achieve high accuracy for the compressibility factor and density of natural gas for custody transfer. It shows good performance and high accuracy for the temperature range between 143.15 K and 676.15 K, and pressure up to 280 MPa. The general form of AGA8 EOS is defined as follows [25]:

$$P = Z\rho_m RT \tag{A1}$$

where Z, ρ_m and R are compressibility factor, molar density and universal gas constant respectively.

In AGA8 method, the compressibility factor should be calculated by employing the following equation [25]:

$$Z = 1 + B\rho_m - \rho_r \sum_{n=13}^{18} C_n^* + \sum_{n=13}^{18} C_n^* D_n^* \tag{A2}$$

Where, ρ_r is reduced density and defined as follows:

$$\rho_r = K^3 \rho_m \tag{A3}$$

where in equation (A3), K is mixture size parameter and calculated using following equation [25]:

$$K^5 = \left(\sum_{i=1}^{N} x_i K_i^{\frac{5}{2}}\right)^2 + 2\sum_{i=1}^{N-1}\sum_{j=i+1}^{N} x_i x_j \left(K_{ij}^5 - 1\right)\left(K_i K_j\right)^{\frac{5}{2}} \tag{A4}$$

In equation (A4), x_i is mole fraction of component i in mixture, x_j is mole fraction of component j in mixture, K_i is size parameter of component i, K_j is size parameter of component j, K_{ij} is binary interaction parameter for size and N is number of component in gas mixture.

In equation (A2), B is second virial coefficient and given by the following equation [25]:

$$B = \sum_{n=1}^{18} a_n T^{-u_n} \sum_{i=1}^{N}\sum_{j=1}^{N} x_i x_j B_{nij}^* E_{ij}^{u_n} \left(K_i K_j\right)^{\frac{3}{2}} \tag{A5}$$

where, B_{nij}^* and E_{ij} are defined by the following equations [25]:

$$B_{nij}^* = \left(G_{ij} + 1 - g_n\right)^{g_n} \left(Q_i Q_j + 1 - q_n\right)^{q_n} \left(F_i^{1/2} F_j^{1/2} + 1 - f_n\right)^{f_n} \times \left(S_i S_j + 1 - s_n\right)^{s_n} \left(W_i W_j + 1 - w_n\right)^{w_n} \tag{A6}$$

$$E_{ij} = E_{ij}^* \left(E_i E_j\right)^{1/2} \tag{A7}$$

In equation (A7), G_{ij} is defined by the following equation [25]:

$$G_{ij} = \frac{G_{ij}^* \left(G_i + G_j\right)}{2} \tag{A8}$$

In equations (A4) to (A8), $a_n, f_n, g_n, q_n, s_n, u_n, w_n$ are the equation of state parameters, E_i, F_i, G_i, K_i, Q_i, S_i,W_i are the corresponding characterization parameters and E_{ij}^*, G_{ij}^* are corresponding binary interaction parameters.

In equation (A2), $C_n^*; n = 1, \ldots, 58$ are temperature dependent coefficients and defined by the following equation [25]:

$$C_n^* = a_n \left(G + 1 - g_n\right)^{g_n} \left(Q^2 + 1 - q_n\right)^{q_n} \left(F + 1 - f_n\right)^{f_n} U_n^{u_n} T^{-u_n} \tag{A9}$$

In equation (A9), G, F, Q, U are the mixture parameters and defined by the following equations [25]:

$$U^5 = \left(\sum_{i=1}^{N} x_i E_i^{\frac{5}{2}}\right)^2 + 2\sum_{i=1}^{N-1}\sum_{j=i+1}^{N} x_i x_j \left(U_{ij}^5 - 1\right)\left(E_i E_j\right)^{\frac{5}{2}} \tag{A10}$$

$$G = \sum_{i=1}^{N} x_i G_i + 2\sum_{i=1}^{N-1}\sum_{j=i+1}^{N} x_i x_j \left(G_{ij}^* - 1\right)\left(G_i + G_j\right) \tag{A11}$$

$$Q = \sum_{i=1}^{N} x_i Q_i \tag{A12}$$

$$F = \sum_{i=1}^{N} x_i^2 F_i \tag{A13}$$

where in equation (A10), U_{ij} is the binary interaction parameter for mixture energy.

In equation (A2), D_n^* is defined by the following equation:

$$D_n^* = \left(b_n - c_n k_n \rho_r^{k_n}\right)\rho_r^{b_n} \exp\left(-c_n \rho_r^{k_n}\right) \tag{A14}$$

Coefficients of equation (35) are introduced in Ref. [25].

Substituting equation (A2) in equation (A1), the temperature, pressure and composition of natural gas are known. The only unknown parameter is molar density. The molar density is calculated using Newton–Raphson iterative method.

The density of natural gas is then calculated by the following equation:

$$\rho = M_w \rho_m \tag{A15}$$

where, M_w is molecular weight of mixture and ρ_m is molar density. With being known molar density, compressibility factor is calculated using equation (A2).

AGA8 model is indented for specific range of the gas components. Table A.1 shows range of gas characteristics to which AGA8 EOS model could be employed [25].

A.1. Computing enthalpy (h)

Assuming enthalpy is functions of temperature and molar specific volume, the enthalpy residual function is defined as follows [39]:

Table A.1
Range of gas mixture characteristics in AGA8 model [20].

Component (mole %)	Normal range	Expanded range
Methane	45 to 100	**0 to 100**
Nitrogen	0 to 50	**0 to 100**
Carbon dioxide	0 to 30	**0 to 100**
Ethane	0 to 10	**0 to 100**
Propane	0 to 4	**0 to 12**
Total butanes	0 to 1	**0 to 6**
Total pentanes	0 to 0.3	**0 to 4**
Hexanes plus	0 to 0.2	**0 to Dew Point**
Helium	0 to 0.2	**0 to 3**
Hydrogen	0 to 10	**0 to 100**
Carbon monoxide	0 to 3	**0 to 3**
Argon	0	**0 to 1**
Oxygen	0	**0 to 21**
Water	0 to 0.05	**0 to Dew Point**
Hydrogen sulfide	0 to 0.02	**0 to 100**

$$h_m - h_{m,I} = \int_{v_{m,I}\to\infty}^{v_m} \left[T\left(\frac{\partial P}{\partial T}\right)_{v_m} - P\right] dv_m + \int_{v_{m,I}\to\infty}^{v_m} RT\left(\frac{\partial Z}{\partial v_m}\right)_T dv_m \tag{A16}$$

In equation (A16), h_m is molar enthalpy for real gas, $h_{m,I}$ molar enthalpy for ideal gas and $v_{m,I}$ is molar specific volume for ideal gas. By changing the variable of v_m to ρ_m and calculation of partial differential values in equation (A16), enthalpy residual function becomes as follows:

$$h_m - h_{m,I} = -RT^2 \int_0^{\rho_m} \left(\frac{\partial Z}{\partial T}\right)_{\rho_m} \frac{d\rho_m}{\rho_m} + RT(Z-1) \tag{A17}$$

Molar enthalpy for ideal gas $h_{m,I}$ could be calculated as follow [39]:

$$h_{m,I} = \sum_{j=1}^{N} x_j h_{m,i}^j \tag{A18}$$

Where in equation (A18), x_j is mole fraction of component j in mixture and $h_{m,i}^j$ is molar enthalpy for ideal gas and for component j in mixture. Coefficients in equation (A18) are given in Ref. [34].

A.2. Computing internal energy (u)

Assuming internal energy is functions of temperature and molar specific volume, the internal energy residual function could be calculated as [39]:

$$u_m - u_{m,I} = -RT^2 \int_0^{\rho_m} \left(\frac{\partial Z}{\partial T}\right)_{\rho_m} \frac{d\rho_m}{\rho_m} \tag{A19}$$

Where, $u_m$is molar internal energy for real gas and $u_{m,I}$ is molar internal energy for ideal gas. Molar internal energy for ideal gas could be calculated using the following equation [40]:

$$u_{m,I} = h_{m,I} - Pv_m = h_{m,I} - RT \tag{A20}$$

In equation (A20), $h_{m,I}$ is molar enthalpy for ideal gas, T is temperature and R is universal gas constant.

References

[1] Farzaneh-Gord M, Rahbari HR, Deymi-Dashtebayaz M. Effects of natural gas compositions on CNG fast filling process for buffer storage system. Oil Gas Sci Technol Rev IFP Energies Nouvelles 2014;69(2):319–30.

[2] Farzaneh-Gord M, Deymi-Dashtebayaz M, Rahbari HR. Optimising compressed natural gas filling stations reservoir pressure based on thermodynamic analysis. Int J Exergy 2012;10(3):299–320.

[3] Stouffs P, Tazerout M, Wauters P. Thermodynamic analysis of reciprocating compressors. Int J Thermodyn Sci 2000;40:52–66.

[4] Armaghani T, Sahebi SA, Goodarzian H. The first law simulation and second law analysis of a typical reciprocating air compressor. Indian J Sci Technol 2012;5(3):2390–5.

[5] Farzaneh Gord M, Niazmand A, Deymi-DashteBayaz M. Optimizing reciprocating air compressor design parameters based on first law analysis. U.P.B. Sci Bull Ser D 2013;75(4).

[6] Farzaneh Gord M, Niazmand A, Deymi-DashteBayaz M, Rahbari HR. Thermodynamic analysis of natural gas reciprocating compressors based on real and ideal gas models. Int J Refrig 2015;56:186–97.

[7] Castaing-Lasvignottes J, Gibout S. Dynamic simulation of reciprocating refrigeration compressors and experimental validation. Int J Refrig 2010;33:381–9.

[8] Porkhial S, Khastoo B, Modarres Razavi MR. Transient characteristic of reciprocating compressors in household refrigerators. Appl Therm Eng 2002;22:1391–402.

[9] Pérez-Segarra CD, Rigola J, Sòria M, Oliva A. Detailed thermodynamic characterization of hermetic reciprocating compressors. Int J Refrig 2005;28:579–93.

[10] Elhaji M, Gu F, Ball AD, Albarbar A. Numerical simulation and experimental study of a two-stage reciprocating compressor for condition monitoring. Mech Syst Signal Process 2008;22:374–89.
[11] Winandy E, Saavedra O, Lebrun J. Simplified modeling of an open-type reciprocating compressor. Int J Sci 2002;41:183–92.
[12] Ndiaye D, Bernier M. Dynamic model of a hermetic reciprocating compressor in on-off cycling operation (Abbreviation: compressor dynamic model). Appl Therm Eng 2010;30:792–9.
[13] Da Riva Enrico, Col David Del. Performance of a semi-hermetic reciprocating compressor with propane and mineral oil. Int J Refrig 2011;34:752–63.
[14] Damle R, Rigola J, Perez-Segarra, Castro J, Oliva A. Object-oriented simulation of reciprocating compressors: numerical verification and experimental comparison. Int J Refrig 2011;34:1989–98.
[15] Negrao Cezar OR, Erthal Raul H, Andrade Diogo EV, da Silva Luciana Wasnievski. A semi-empirical model for the unsteady-state simulation of reciprocating compressors for household refrigeration applications. Appl Therm Eng 2011;31:1114–24.
[16] Ma Yuan, He Zhilong, Peng Xueyuan, Ziwen Xing. Experimental investigation of the discharge valve dynamics in a reciprocating compressor for trans-critical CO_2 refrigeration cycle. Appl Therm Eng 2012;32:13–21.
[17] Hajbabaeia M, Karavalakisa G, Johnsona K, Lee L, Durbina T. Impact of natural gas fuel composition on criteria, toxic, and particle emissions from transit buses equipped with lean burn and stoichiometric engines. Energy 2013;62:425–34.
[18] Karavalakisa G, Hajbabaeia M, Durbina T, Johnsona K, Zheng Zh, Miller W. The effect of natural gas composition on the regulated emissions, gaseous toxic pollutants, and ultrafine particle number emissions from a refuse hauler vehicle. Energy 2013;50:280–91.
[19] Burlutskiy E. Mathematical modelling on rapid decompression in base natural gas mixtures under rupturing. Chem Eng Res Des 2013;9(1):63–9.
[20] Kakaee A, Paykani A, Ghajar M. The influence of fuel composition on the combustion and emission characteristics of natural gas fuelled engines. Renew Sustain Energy Rev 2014;38:64–78.
[21] AGA8–DC92 EoS. Compressibility and super compressibility for natural gas and other hydrocarbon gases. 1992. Transmission Measurement Committee Report No. 8, AGA Catalog No. XQ 1285, Arlington, VA, https://www.aga.org.
[22] ISO-12213-2. Natural Gas calculation of compression factor-part 2: calculation using molar-composition analysis. ISO; 1997. Ref. No. ISO-12213-2:1997(E).
[23] Farzaneh-Gord M, Rahbari HR. Numerical procedures for natural gas accurate thermodynamics properties calculation. J Eng Thermophys 2012;21(4):213–34.
[24] National Iran Gas Company official website, http://NIGC.com/pages/Products.htm.
[25] Lee Sukhyung. First law analysis of unsteady processes with application to a charging process and a reciprocating compressor. The Ohaio State University; 1983. A Thesis presented in Partial Fulfillment of the Requirements for Degree of master Science.
[26] Brablik J. Gas pulsations as a factor affecting operation of automatic valves in reciprocating compressors. In: Proceeding of purdue compressor technology conference; 1972. p. 188–95.
[27] Srinivas MN, Padmanabhan Ch. Computationally efficient model for refrigeration compressor gas dynamics. Int J Refrig 2002;25:1083–92.
[28] Singh R. Modeling of multi cylinder compressor discharge systems [PhD thesis]. Purdue University; 1975.
[29] Boswirth L. Flow forces and the tilting of spring loaded valve plates. In: Proceedings of the purdue compressor conference; 1980. p. 185–97.
[30] Adair RP, Qvale EB, Pearson JT. Instantaneous heat transfer to the cylinder wall in reciprocating compressors. In: Purdue compressor technology conference Proc.; 1972. p. 521–6.
[31] Richard Stone. Introduction to internal combustion engines. Department of Engineering Science, University of Oxford; 1999.
[32] Hatami M, Ganji DD, Gorji-Bandpy M. A review of different heat exchangers designs for increasing the diesel exhaust waste heat recovery. Renew Sustain Energy Rev 2014;37:168–81.
[33] Hatami M, Jafaryar M, Ganji DD, Gorji-Bandpy M. Optimization of finned-tube heat exchangers for diesel exhaust waste heat recovery using CFD and CCD techniques. Int Commun Heat Mass Transf 2014;57:254–63.
[34] Hatami M, Ganji DD, Gorji-Bandpy M. Numerical study of finned type heat exchangers for ICEs exhaust waste heat recovery. Case Study Therm Eng 2014;4:53–64.
[35] Hatami M, Ganji DD, Gorji-Bandpy M. Experimental investigations of diesel exhaust exergy recovery using delta winglet vortex generator heat exchanger. Int J Therm Sci July 2015;93:52–63.
[36] Hatami M, Ganji DD, Gorji-Bandpy M. Experimental and thermodynamical analyses of the diesel exhaust vortex generator heat exchanger for optimizing its operating condition. Appl Therm Eng 22 January 2015;75:580–91.
[37] Ghazikhani M, Hatami M, Ganji DD, Gorji-Bandpy M, Behravan A, Shahi Gh. Exergy recovery from the exhaust cooling in a DI diesel engine for BSFC reduction purposes. Energy 1 February 2014;65:44–51.
[38] Govidan N, Jayaraman V, Venkatasamy S, Ramasamy M. Mathematical modeling and simulation of a reed. Therm Sci 2009;13(3):47–58.
[39] Moran MJ, Shapiro HN. Fundamentals of engineering thermodynamics. 6th ed. Wiley; 2007, ISBN 0471787353.
[40] DIPPR® 801. Evaluated standard thermophysical property values. Design Institute for Physical Properties; 2004. Sponsored by AIChE.

Nomenclature

a: lengths of rod m
A: area (m^2)
C_d: orifice discharge coefficient
c_p, c_v: constant pressure &volume specific heats (kJ/kg K)
g: gravitational acceleration (m/s^2)
h: specific enthalpy (kJ/kg)
L: crank m
$\dot{m}$: mass flow rate (kg/s)
M: molecular weight (kg/kmol)
P: pressure (bar or Pa)
$\dot{Q}$: heat transfer rate (kW)
S: stroke m
T: temperature (K or °C)
u: internal energy (kJ/kg)
υ: specific volume (m^3/kg)
V: volume (m^3)
V_0: dead volume (m^3)
v: velocity (m/s)
W: actual work (kJ/kg)
$\dot{W}$: actual work rate (kW or MW)
x: displacement (m)
z: height (m)
$+C_6$: all hydrocarbon compounds with more than 5 carbon in their chemical formula
ρ: density (kg/m^3)
ω: angular Speed (rad/s)
α: heat Transfer Coefficient (Wm^2/K)
θ: degree (degree)

Subscript

d: discharge condition
cv: control volume condition
s: suction condition
p: piston

Greek Letters

ρ_m: molar density
ρ_r: reduce density
γ: gas gravity
ν_m: molar specific volume